

Received March 26, 2022, accepted April 21, 2022, date of publication April 29, 2022, date of current version May 6, 2022.

Digital Object Identifier 10.1109/ACCESS.2022.3171255

Impact of Bandwidth on Range Resolution of Multiple Targets Using Photonic Radar

**ABHISHEK SHARMA¹, (Graduate Student Member, IEEE),
SUSHANK CHAUDHARY², (Senior Member, IEEE), JYOTEESH MALHOTRA¹,
AMIR PARNIANIFARD², SANTOSH KUMAR³, (Senior Member, IEEE),
AND LUNCHAKORN WUTTISITTIKULKIJ², (Senior Member, IEEE)**

¹Department of Electronics Technology, Guru Nanak Dev University, Regional Campus, Punjab 144007, India

²Department of Electrical Engineering, Wireless Communications Ecosystem Research Unit, Chulalongkorn University, Bangkok 10330, Thailand

³Shandong Key Laboratory of Optical Communication Science and Technology, School of Physics Science and Information Technology, Liaocheng University, Liaocheng 252000, China

Corresponding authors: Sushank Chaudhary (sushankchaudhary@gmail.com) and Lunchakorn Wuttisittikulki (lunchakorn.w@chula.ac.th)

This work was supported in part by the Second Century Fund (C2F), Chulalongkorn University, Thailand, and in part by the Thailand Science Research and Innovation Fund Chulalongkorn University under Grant CU_FRB65_ind (12)_160_21_26.

ABSTRACT Futuristic transportation systems would be requiring more effective sensing system that are not only cost effective but also more efficient in sensing multiple targets while acquiring minimal area and utilizing low input power. To achieve that, frequency modulated continuous wave (FMCW) based Photonic Radar is proposed. For multiple targets detection, wavelength division multiplexing (WDM) scheme is used in conjugation with polarization division multiplexing (PDM) scheme. Impact of varying bandwidth is analyzed upon the performance of the proposed system using numerical simulations. The system is simulated for detecting and ranging over 100 meters by analyzing received echoes and verifying the range frequency with theoretically calculated values while effective operation is measured in terms of received power under varying level of attenuation up to 75 dB/Km under rain and fog conditions. Lastly, the system is replicated for range resolution with four varying operational bandwidths from 600 MHz to 4 GHz.

INDEX TERMS Frequency modulated continuous wave (FMCW), photonic radar, polarization division multiplexing (PDM), wavelength division multiplexing (WDM).

I. INTRODUCTION

Intelligent transportation systems are expected to be integral part of smart cities where self-driving vehicles not only transport but also make decisions in driverless operation on the lanes [1]. Among the advantages accessible through self-driving vehicles, radical lessening in fatal road mishaps is expected along with decrease in CO₂ emission, lower fuel consumption, reduced lane congestion and efficient and economical transportation [2]. Despite the cost, several challenges common to all self-driving vehicles are worth considering for realizing intelligent transportation. The accident in 2016 of prototype launched by Tesla [3] led to wide speculation of feasibility of such driverless system as well as its reliability and accountability in case of misshaping. Other issue is to safeguard electronic operating system in autonomous vehicles from being hacked or misused

The associate editor coordinating the review of this manuscript and approving it for publication was Tianhua Xu¹.

by miscreants. Different sensors work together to enable a complete intelligent transportation including cameras, ultrasonic sensors, Photonic radar, artificial intelligence and GPS (Global Positioning System). Therefore, to avoid collision and successful detection and tracking of different targets, both high and low budget self-driving vehicles need to access high volume of data in terabytes per hour and hence higher data rate poses another challenge in realization of intelligent transportation system [4].

Existing navigation and observation devices based upon microwave technology have inadequate precision-range particularly in densely congested places [5], [6] even at higher frequencies. Initially, Radar operations were carried out using 24 GHz frequency band [7] thus having limited bandwidth available which limits the range resolution and detection capability under the adverse atmospheric condition hence AV industry has shifted towards higher frequency band of 77 GHz with larger available bandwidth for AVs operations at 77 – 81 GHz band, also termed as short range

radar (SRR) band. However, SSR band suffers austere attenuations specifically under the inconsistent climatic conditions such as cloudy, foggy, rainy and snowy [8]. Other atmospheric constituents such as vapours and rudiments attenuate mm-band signal by absorption. This results in weakening of the target detection and range resolution and hence minimal indicators are attained for decision making [9]. Sufficient literature is available reporting the impact of atmospheric turbulences operating in free space optics environment and many researchers have studied these impacts of various random atmospheric disparities upon the intelligent transportation using different simulation methods [10]. The impact of attenuation on performance of time of flight (ToF) based rangefinder using laser at different wavelengths is reported [11]. The time-of-flight operation is a state of art technology and readily applied in Photonic radars. However, FMCW-based Photonic radar offers advantages such as enhanced resolution and precision in ranging along with its compact size and minimal power requirement as compared with the conventional time-of-flight radar [12]. Generally, 1550 nm wavelength is preferred in AVs for operation as it is safe for humans. High vulnerability towards moisture, rain and fog is anticipated at this wavelength due to water absorption. Other studies [13]–[15] confirm impact of atmospheric variations upon Photonic radar in presence of disperse gases, rain, fog and temperature deviations. Nevertheless, these reported works considered single target detection in normal traffic situations. Thus, the prominence of Frequency modulated continuous waves-based Photonic radar system upsurges considerably and is swiftly developing at its early stages by delivering accuracy in range resolution as well as prolonged detection range [16], [17].

Furthermore, some studies have been reported in surveillance linked usages under complex traffic conditions such as [18] reported mm-wave based radar to distinguish amid infrastructures and moving automobiles using algorithm-based approach in 24 GHz band. Another study utilises interferometry method [19] in 35 GHz band to measure vehicle speed in complex targets scenario to distinguish between moving targets, but the system fails to distinguish when two targets move at the same speed. Further, the atmospheric influence on AVs is not included in the reported works [18], [19]. Recently, a fusion between photonic-based radar and FMCW-based Photonic radar is also proposed [20] and reported results show enhanced range resolution but the study is limited to single target and in clear atmospheric conditions. Also, the impact of atmospheric turbulence on the direct detection and coherent detection-based FMCW sensors is proposed but with single target [21]–[23].

In this paper, deliberations are focused on the target detections and ranging in complex traffic scenario considering multiple vehicles using Photonic radar and ability of the proposed sensor in distinguishing between closely placed targets. Another issue is low power availability from vehicles battery as well as minimal dimensions of sensor so as to give more flexibility to vehicle designer. Hence, the paper

is focused towards developing low cost and low dimensions (also known as SWAP) based basic features needed for self-driving vehicles.

For ease of procedure, linear frequency modulated continuous wave radar system using direct detection configuration (FMCW-DD) has been used in Photonic radar system. In FMCW-DD system, transmitted pulse is intensity modulated by LFM chirp and de-chirping is accomplished by comprehensible mixing with a modulated local oscillator (LO) [24], [25]. The system is simulated for multiple targets detection using eight targets in direct detection configuration and under the impact of severe atmospheric conditions. To enable multiple targets detection, polarization division multiplexing (PDM) in conjugation with wavelength division multiplexing (WDM) has been employed in the proposed Photonic radar sensor system. The PDM inclusion ensures enormous working frequency range and better sturdiness in the operation of Photonic radar system as neither precise high modulation index nor optical filtering is required [26], [27]. The system is also simulated for range resolution using different frequency bandwidths under adverse weather conditions and results were compared as effected of varying bandwidth on the range resolution of Photonic radar. The contributions of the proposed Photonic radar system in this paper are briefed as follows:

- Designing a small and low-cost Photonic radar system
- Testing the system under adverse weather conditions using eight targets as complex traffic scenario
- Evaluating the impact of bandwidth variations in detection as well as on range resolution of multiple targets

The rest of the paper is structured as follows. Section II deliberates working principle and modelling of the proposed Photonic radar sensor system. Section III presents and discusses the theoretically verified results under different atmospheric conditions as well as bandwidth variations. Section IV concludes the paper.

II. WORKING PRINCIPLE AND SYSTEM MODEL

Figure 1 exhibits the structure of the FMCW-based photonic radar sensor system in direct detection formation also known as homodyne formation. The system modelled with low input power requirements as well as compact design to comply with AVs power and design necessities. The system uses triangular sweep [28] as it offers minimal sweep time in triangulation of objects than the pulsed sweep. A pseudo random signal is generated with a bit rate of 90 Kbps and fed into the saw-tooth wave generator. The saw-tooth generator converts input sequence into triangular signal with the sample rate of 819.19 Mbps having maximum amplitude of 1 a.u. This triangular sweep measures the frequency inconsistency in approximation of target range as well as for interim period between transmitted signal and received echo. The triangular signal is then fed into linear frequency modulator (LFM) with start frequency of 77 GHz. Considering the f_c as start frequency, B as bandwidth, R as distance between target and

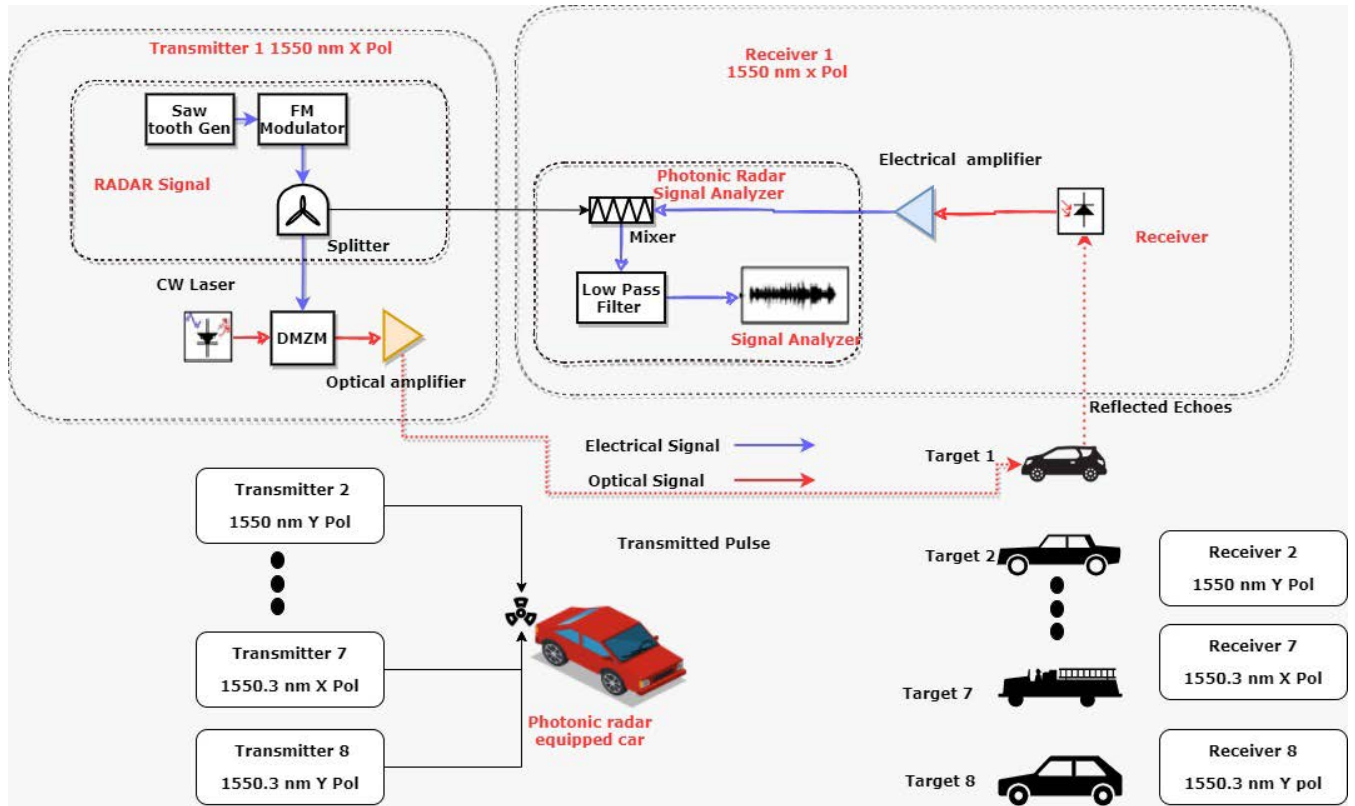


FIGURE 1. Block diagram of proposed FMCW based Photonic radar sensor system for intelligent transportation system. CW: Continuous wave; APD: avalanche photo diode and λ is wavelength used.

sensor equipped vehicle and T_m as sweep time, the range frequency f_r at which echo signal occurs is calculated by using [29]:

$$f_r = \frac{(2 \times R \times B)}{(T_m \times c)} \quad (1)$$

where, c is speed of light. The sweep rate of frequency and round trip time of local oscillator are matched in order to accomplish higher quality factor [30].

To power eight transmitters, four optical continuous wave (CW) laser sources have been employed with input power of 0 dBm and linewidth of 0.1 MHz while four wavelengths are employed with 0.1 nm channel spacing i.e., 1550 nm, 1550.1 nm, 1550.2 nm and 1550.3 nm. The optical output of CW laser and radio frequency output of LFM generator is then modulated together using lithium niobate (Li-Nb) dual arm Mach-Zehnder (DM-MZM) external modulator. DM-MZM has the extinction ratio of 30 dB and switching bias voltage of 4v. DC bias is also used with DM-MZM to subdue any additional bands and to produce second order bands. The transfer function of the DM-MZM is given as [31]:

$$\frac{E_{out}}{E_{in}} = \cos\left(\phi_o + \frac{\pi S(t)}{2V_\pi}\right) \quad (2)$$

where, ϕ_i is the primary phase, v_π is the power needed to transform the optical power transfer function, E_{out} and E_{in}

are input and output optical fields, and $S(t)$ is the LFM signal strength given as [32]:

$$S(t) = A_c \cos(2\pi f_c t + \frac{\pi B}{T_m} t^2) \quad (3)$$

where, A_c is the amplitude, B is the sweep bandwidth and f_c is the start frequency. For homodyne detection systems, MZM output power is expressed as in equation 4 [32]:

$$E_{Tx}(t) = \sqrt{\frac{P_t}{2}} [1 + \frac{\beta}{2} \cos(2\pi f_c t + \frac{\pi B}{T_m} t^2)]. e^{j(\omega_o t + \theta_o(t))} \quad (4)$$

where $\theta_o(t)$ is the arbitrary phase element, ω_o is the angular frequency and β is the modulation index ($\beta \ll 1$). The output modulated signal is fed into polarization controller where state of polarization is given to the optically modulated LFM signal. For simplicity of operation, odd channels (channel 1, 3, 5 and 7) are multiplexed together, given 0° phase shift depicted as X polarization and even channels (channel 2, 4, 6 and 8) multiplexed together, given 90° phase shift depicted as Y polarization as shown in figure 1. The polarised signal from X and Y polarization states is combined using power combiner and this polarized-multiplexed signal is then amplified using optical amplifier signal having 10 dB gain and 4 dB of noise figure. The amplified signal then focuses on the multiple targets using telescope lens with aperture size of 5 mm and 15 mm via free space channel. Various elements affect the echo signal reflected from the target to the receiver

such as reflectivity of target, atmospheric effects and angular dispersion.

At the receiver section, the signal is separated using polarization splitter again as X and Y polarized signal followed by a de-multiplexer. The power received from the echo signal P_r is given as in equation 5 [29]:

$$P_r = \begin{pmatrix} P_t \frac{\rho_t D^2 \tau_{opt} \tau_{atm}^2}{4R^2} & \text{for any extended target} \\ P_t \frac{\rho_t A_t D^2 \tau_{opt} \tau_{atm}^2}{4R^2 A_{ill}} & \text{for any target} \end{pmatrix} \quad (5)$$

where ρ_t is the target reflectivity, A_t is the target area, R is the target range, D is the receiver aperture diameter, τ_{opt} is the transmission loss in the optical domain, τ_{atm} is the atmospheric loss factor and A_{ill} is the illuminated area at target. The resonated signal power E_{ref} at receiver is given as [29]:

$$E_{ref}(t) = \sqrt{P_r} \left[1 + \frac{\beta}{2} \cos(2\pi f_c(t - \tau)) + \frac{\pi B}{T_m} (t - \tau)^2 \right] e^{j(\omega_o - \omega_d)t + \theta_o(t)} \quad (6)$$

where, τ is the propagation delay given as $\tau = 2 \times R/c$. As optical mixing of signal is not done in homodyne detection, photodiode output having the responsivity \Re is expressed as [33]:

$$i_{ph}(t) = \Re.P_r \left(1 + \frac{\beta}{2} \cos(2\pi f_c(t - \tau)) + \frac{\pi B}{T_m} (t - \tau)^2 \right)^2 \quad (7)$$

And filtered photocurrent signal to acquire baseband signal given as [32]:

$$i_{ph}(t) = I_{dc} + i_{sig}(t) \approx \Re.P_r \left(1 + \frac{\beta}{2} \cos(2\pi f_c(t - \tau)) + \frac{\pi B}{T_m} (t - \tau)^2 \right)^2 \quad (8)$$

where I_{dc} and i_{sig} are dc and ac current signals obtained from the photo detector.

Photodetector used to detect echoes signal in this sensor system is PIN type with dark current noise of 10 nA and bandwidth of 0.4 GHz having device limitations such as shot noise, thermal noise and amplified spontaneous emission. The constant responsivity of engaged PIN type photodetector is 1 A/W. The system is evaluated in terms of received power and measured signal to noise ration using electrical analyser after the photo-detector as given in equation 9 [29]:

$$SNR_{dir} = \frac{\beta^2 \Re^2 P_r^2 / 2}{q \Re P_r B_{rx} + 4k_b T_r B_{rx} / RL} \quad (9)$$

where k_b is the Boltzmann constant $\approx 1.38 \times 10^{-23}$ J/K, q is the electrical charge $\approx 1.6 \times 10^{-19}$ c, T_r is the receiver noise temperature, RL is the load resistance and B_{rx} is the receiver bandwidth.

The detected signal from the photodetector is then amplified using electrical amplifier with the gain of 40 dB and fed into the mixer where signal from LFM is mixed with received and amplified signal. The mixed signal is then subjected to the low pass filter (LPF) having the cut-off frequency

TABLE 1. Photonic radar modeling parameter.

Component	Parameter	Value
Continuous wave laser	Wavelength	1550 – 1550.3 nm
	Channel Spacing	0.1 nm
	Linewidth	100 KHz
	Power	100 μ W
Dual Port Mech-Zehnder modulator (DP-MZM)	Extinction ratio	30 dB
	Switching bias voltage	4 v
	Switching RF voltage	4 v
	Bias voltage	0 v
Photo detector (PIN)	Responsivity	1 A/W
	Dark Current	1 nA
	Thermal and shot noise BW	410 MHz
	Absolute temp	290k
	Load resistance	50 Ω

μ s = micro-second, nm = Nano meter, KHz/MHz = Kilo Hertz/Mega Hertz, μ W = micro-watt, dB = decibel, v = volts, A/W = ampere per watt, k = kelvin and Ω = ohms.

of 1 GHz. The beat signal produced by the LPF is given as in equation 10 [29]:

$$S_b(t) = A_c \Re P_r \beta \cos(2\pi f_c \tau - \frac{\pi B}{T_m} \tau^2 + 2\pi f_r t) \quad (10)$$

The filtered signal from LPF is then analysed for detection using RF spectrum analyser where the range frequency is observed. The parameters considered for Photonic radar sensor are mentioned in Table 1.

III. RESULTS AND DISCUSSION

An all-inclusive discussion is presented in this section which describes the results acquired from the proposed Photonic radar sensor. The gleaming is assumed to be ideal in the atmospheric channel. As mentioned in table 1, a total of 8192 samples were considered during modelling of the proposed sensor system. The system is modelled to detect and range multiple targets as shown in figure 1.

As the sensor system is designed to analyse impact of bandwidth variations and detection and range resolution, the system is simulated with 4 bandwidths, i.e., 600 MHz, 1 GHz, 2GHz and 4 GHz. Firstly, the system is simulated with clear weather conditions as shown in Figure 2. The range frequency peaks obtained from RF spectrum analyser using the proposed Photonic radar sensor show same frequency value as calculated using equation 1 theoretically. For instance, with bandwidth of 600 MHz, the range frequency at 100 meters should be 40 MHz, with bandwidth 1 GHz it should be 66.66 MHz and with bandwidth 4 GHz it should be 266.66 MHz. By observing Figure 2, it can be seen that peak is obtained at the same values for echo signal. The system results in successful detection and ranging of all the targets with acceptable power levels. As autonomous vehicles are thought to be efficient under adverse atmospheric conditions, hence Photonic radar sensor must be able to detect and range under the influence of strong turbulences such as rain and fog. Impacts of these turbulences are deterrent and result in

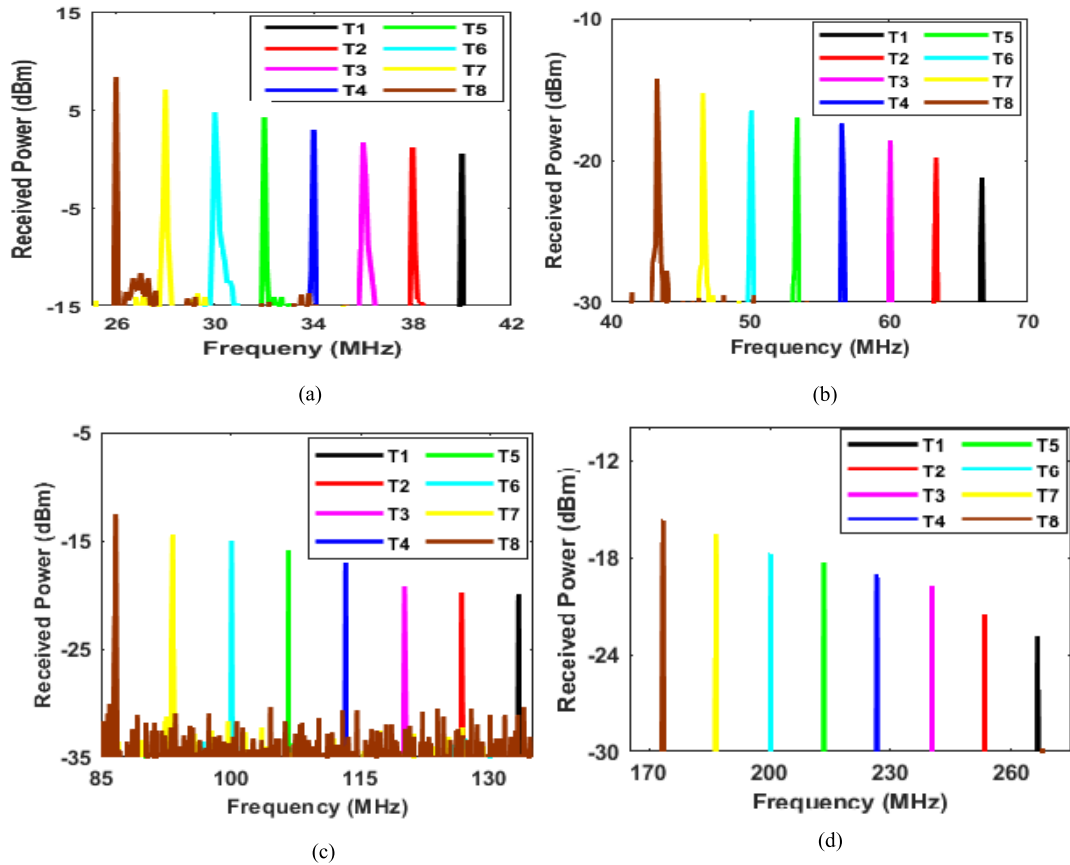


FIGURE 2. Reflected Echoes obtained from multiple targets using bandwidth (a) 600 MHz, (b) 1 GHz, (c) 2 GHz and (d) 4 GHz under clear conditions. T1: Target1 at 100 meters; T2: Target 2 at 95 meters; T3: Target 3 at 90 meters; T4: Target 4 at 85 meters; T5: Target 5 at 80 meters; T6: Target 6 at 75 meters; T7: Target 7 at 70 meters; T8: Target 8 at 65 meters.

zero visibility which can be hazardous for the operation of intelligent transportation systems particularly in mm-wave band. Rain effects are minimal as compared to fog on the operations of Photonic radar as droplet size is large compared to the optical wavelength. Attenuation due to rain A_{rain} can be calculated as given in equation 11 [34]:

$$A_{rain} = k.R_o^\alpha \tag{11}$$

where rate of rainfall is given as R_o in mm/hr while k and α are power law factors which are based upon frequency, temperature and droplet size of the rain. The values of k and α are calculated using Marshal–Palmer distribution [35], [36]. Fog is a mixture of rudiments that degrade the overall system performance particularly at high frequency bands [37]. The impact of fog in terms of attenuation is calculated using Kim’s model based upon Mie scattering given as in equation 12 [38], [39]:

$$\beta(\lambda) = \frac{3.91}{V} \left(\frac{\lambda}{550}\right)^{(-\rho)} \tag{12}$$

where ρ refers to the size distribution coefficient of scattering V the visibility (kms) and λ refers to the operating wavelength of the laser. For modelling purpose, the standard international visibility code values of rain and fog

attenuation adopted from Awan *et al.* [39] are considered in this work in such that light rain or mist with precipitation of 2 mm/hr is considered as 2 dB/km; average rain with 12.5 mm/hr precipitation is considered as 4.6 dB/km; strong rain with 25 mm/hr precipitation is considered at 6.9 dB/Km and storm/snow or light fog with 100 mm/hr precipitation is considered at 18.3 dB/km of attenuation level, respectively. Likewise, moderate fog is considered having 28.9 dB/km of attenuation while thick fog at 75 dB/km of attenuation. Figure 3 represents echoes obtained from multiple targets under the impact of thick fog with attenuation of 75 dB/Km. Other losses viz atmospheric losses, propagation losses and geometric losses are also considered to replicate real-world scenario while analysing atmospheric effects.

It is concluded from the illustrated results that the proposed Photonic radar sensor system has successfully detected and ranged multiple targets under heavy attenuation. The peaks observed in Figure 3 are placed at the same value of frequency in clear weather, but the power level decreased as atmospheric conditions changed.

The actual signal strength of the echo signal received at the photo detector is perceived via electrical analyzer prior to the amplification under the varying values of attenuation

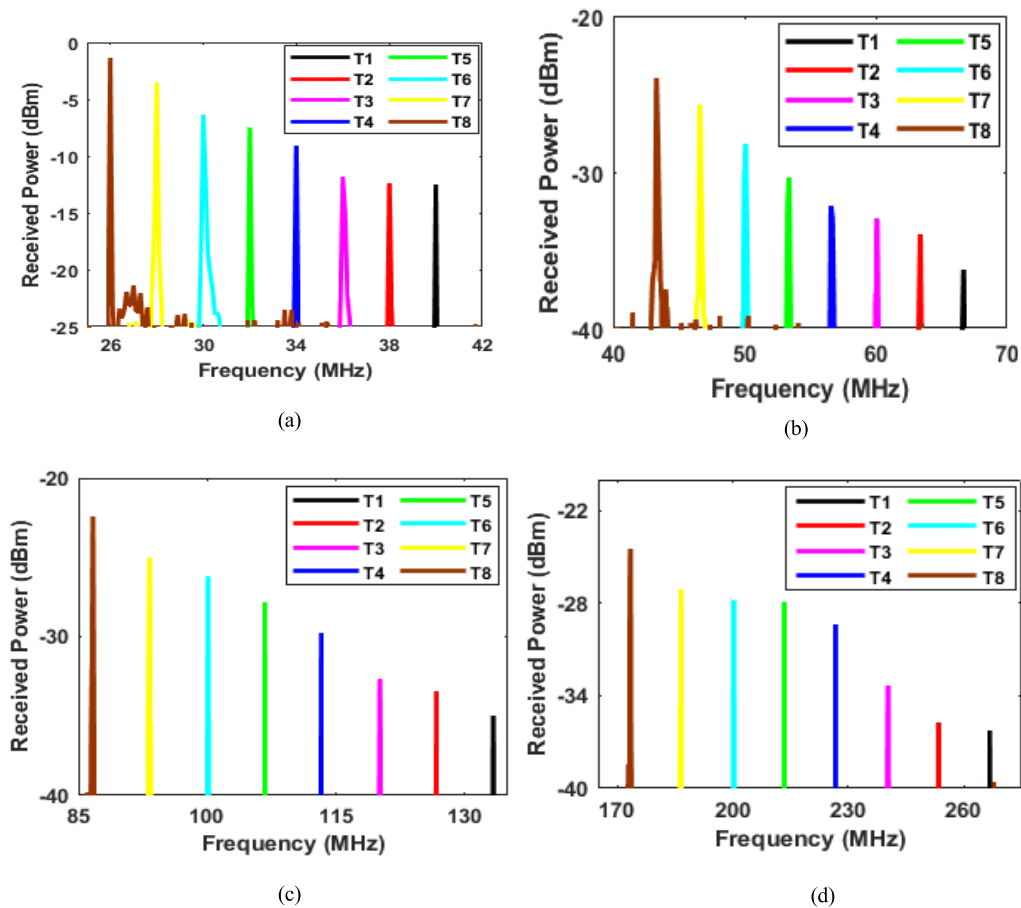


FIGURE 3. Reflected Echoes obtained from multiple targets using bandwidth (a) 600 MHz, (b) 1 GHz, (c) 2 GHz and (d) 4 GHz under thick fog conditions with attenuation 75 dB/km. T1: Target1 at 100 meters; T2: Target 2 at 95 meters; T3: Target 3 at 90 meters; T4: Target 4 at 85 meters; T5: Target 5 at 80 meters; T6: Target 6 at 75 meters; T7: Target 7 at 70 meters; T8: Target 8 at 65 meters.

as defined above. Figure 4 illustrates analogous observed values of received power with respect to varying attenuation up to 70 db/Km with bandwidth of 600 MHz, 1 GHz, 2GHz and 4 GHz, respectively. For instance, power levels of signal observed using 600 MHz bandwidth range between -40 dBm and -60 dBm under varying attenuation levels as illustrated in Figure 4 (a). Likewise, the power levels of received echo signal with 1 GHz bandwidth range between -55 dBm and -80 dBm as shown in figure 4 (b), -58 dBm to -80 dBm with bandwidth 2 GHz as shown in Figure 4 (c) and -61 dBm to -82 dBm using 4 GHz of bandwidth. The minimum detectable power is well within specified acceptable ranges which further strengthen successful detection and ranging of the proposed sensor system.

Likewise, Figure 5 presents the signal to noise ratio curve for all the targets with respect to the attenuation at 4 GHz bandwidth. The reported results depict successful detection of all the targets with acceptable signal to noise ratio.

Another challenge in autonomous vehicles segment is the ability to distinguish between closely spaced targets such as two vehicles moving parallel to avoid any hazardous

condition known as range resolution. The range resolution L_{RES} is defined using equation 13 [40]:

$$L_{res} = \frac{c}{2B} \tag{13}$$

where, B is bandwidth of the system and c is speed of the light. As it is theoretically evident that higher bandwidth means greater resolution using equation 13, the results obtained for range resolution using 600 MHz, 1 GHz, 2GHz and 4 GHz bandwidth are presented in Figure 6. Theoretically, using equation 13 the value for range resolution at 600 MHz bandwidth is obtained as 25 cm. However, while using simulations, as number of closely spaced targets increases, the resolution depletes. For the proposed sensor system, range resolution using 600 MHz is obtained at 75 cm between targets from a ranging distance of 100 meters. Similarly, the theoretical value of range resolution using 1 GHz bandwidth is 15 cm, using bandwidth of 2 GHz its 7.5 cm while using 4 GHz bandwidth resolution is calculated as 3.75 cm. While simulating the scenario with 1 GHz bandwidth, individual peaks are obtained with an inter target distance of 50 cm as observed from 100 meters distance from the Photonic

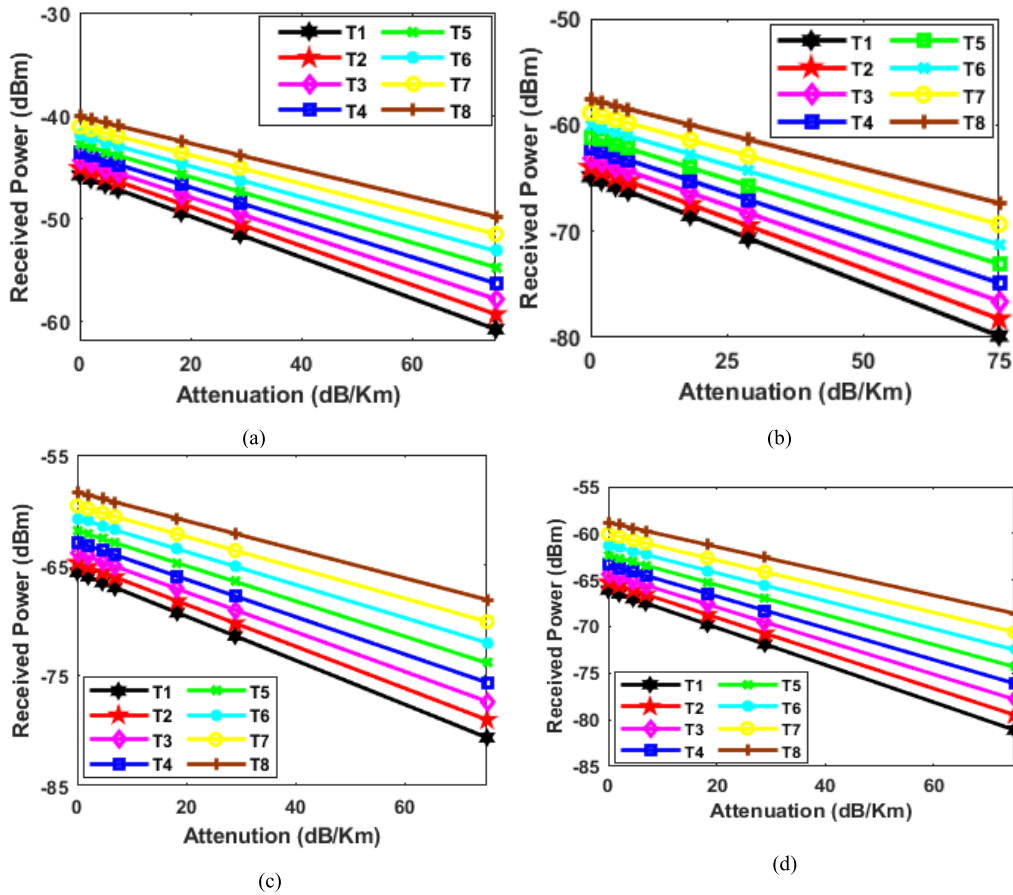


FIGURE 4. Received power with respect to varying attenuation levels at (a) 600 MHz, (b) 1 GHz, (c) 2 GHz and (d) 4 GHz of bandwidth. T1: Target1 at 100 meters; T2: Target 2 at 95 meters; T3: Target 3 at 90 meters; T4: Target 4 at 85 meters; T5: Target 5 at 80 meters; T6: Target 6 at 75 meters; T7: Target 7 at 70 meters; T8: Target 8 at 65 meters.

radar sensor-equipped vehicle which comes down to 40 cm with 2 GHz of bandwidth while the distance between targets comes down to 25 cm with 4 GHz of bandwidth at the same ranging distance of 100 meters between Photonic radar sensor and targets.

As shown in Figure 6 (a), the position of Target 1 is at 100 meters, while the positions of targets 2, 3 and 4 are at 99.25 meters, 98.50 meters and 97.75 meters, respectively. Likewise, Target 5 is placed at 90 meters while targets 6, 7 and 8 are at 90.75 meters, 91.50 meters and 92.25 meters, respectively. Accordingly in Figure 6 (b), the position of targets is displaced by 50 cm such that Target 1 is placed at 100 meters while targets 2, 3 and 4 are at 99.50 meters, 99 meters and 98.50 meters, respectively. While Target 5 is at 90 meters and targets 6, 7 and 8 are at 90.50 meters, 91 meters and 91.50 meters, respectively. In figures 6 (c) and (d) displacement of 40 cm and 25 cm is given in the target position such that for Figure 6 (c) Target 1 is at 100 meters and targets 2, 3 and 4 are at 99.60 meters, 99.20 meters and 98.80 meters, respectively. While Target 5 at 90 meters and targets 6, 7 and 8 are at 90.40 meters, 90.80 meters and 91.20 meters, respectively. Similarly for Figure 6 (d) Target 1 is at 100 meters and targets 2, 3 and 4 are at 99.75 meters, 99.50 meters and

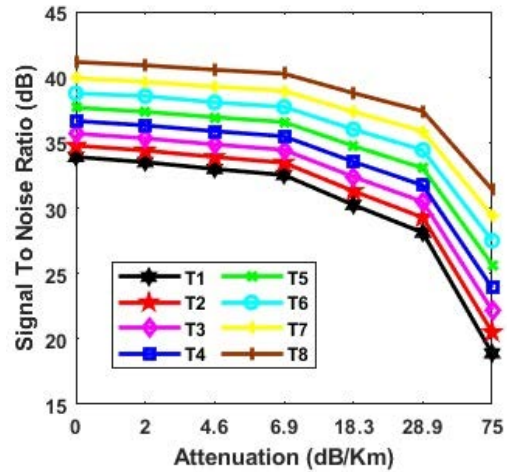


FIGURE 5. Signal to noise ratio with respect to varying attenuation levels at 4 GHz of bandwidth. T1: Target1 at 100 meters; T2: Target 2 at 95 meters; T3: Target 3 at 90 meters; T4: Target 4 at 85 meters; T5: Target 5 at 80 meters; T6: Target 6 at 75 meters; T7: Target 7 at 70 meters; T8: Target 8 at 65 meters.

99.25 meters, respectively. While Target 5 is at 90 meters and targets 6, 7 and 8 are at 90.25 meters, 90.50 meters and 90.75 meters, respectively.

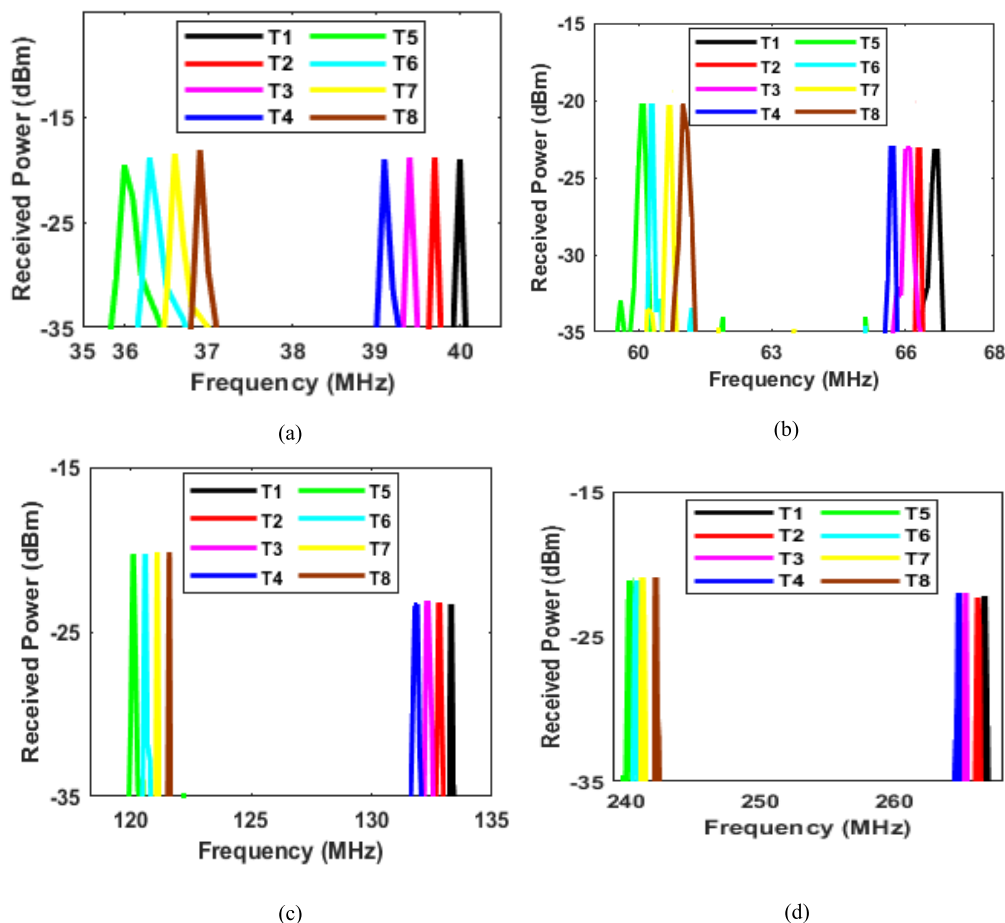


FIGURE 6. Received power spectrum of multiple targets separated by (a) 75 cm at 600 MHz, (b) 50 cm at 1 GHz, (c) 40 cm at 2 GHz and (d) 25 cm at 4 GHz of bandwidth.

TABLE 2. Comparison with recent works.

Operating Band	Detection Range	Range Resolution	Attenuation/Turbulences	No of Targets	Ref
24 GHz and 77 GHz	15 m	n.r. ^a	n.r. ^a	1	[41]
9.7 GHz	25 m	10 cm	Not Considered	1	[42]
77 GHz	550m-heavy fog 1200 m-mild fog >1600-heavy rain	n.r. ^a	Heavy Fog, Mild Fog and Heavy Rain	1	[43]
40 GHz	110 cm	n.r. ^a	n.r. ^a	1	[44]
n.r. ^a	75.6 m	1.375	n.r. ^a	3	[45]
8.5 GHz to 12.5 GHz	1.73 m	5.9 cm	n.r. ^a	1	[46]
77 GHz	100 m	25 cm	Heavy Fog	8	This work

^anot reported

The present work surpasses previously reported works in terms of number of targets detected simultaneously, performance under atmospheric conditions, detection range as well as range resolution as shown in Table 2.

The non-overlapping and strong crests of echoes received from the targets designate the ranging and discovery of all the eight objects at a distance of ~ 100 meters from the sensor system. This points toward the recognition of intelligent transportation system that can differentiate narrowly

located targets. Simulated results depict that the system suffers an error of 50 cm in case of 600 MHz bandwidth; 35 cm in case of 1 GHz bandwidth and 21.25 cm error in case of 4 GHz bandwidth from the hypothetically calculated values.

IV. CONCLUSION

In this work, multiple targets detection is achieved by employing FMCW-based Photonic radar sensor system using PDM-WDM multiplexing to realize an intelligent

transportation system. Different wavelengths were compared for Photonic radar operations. The system is evaluated under the impact of rain and fog with maximum attenuation of 75 dB/km and successful detection and ranging of all the targets is reported at 100 meters from the Photonic radar sensor. The results are validated by observing minimum acceptable received power at photoreceptor for successful sensing operation. Lastly, the sensor system is simulated for range resolution using different wavelengths. The reported results show that the range resolution improves significantly from 75 cm in case of 600 MHz to 25 cm with 4 GHz of bandwidth.

REFERENCES

- [1] F. T. El-Hassan, "Experimenting with sensors of a low-cost prototype of an autonomous vehicle," *IEEE Sensors J.*, vol. 20, no. 21, pp. 13131–13138, Jun. 2020.
- [2] P. Goldin. *10 Advantages of Autonomous Vehicles*. Jun. 30, 2021. [Online]. Available: <https://www.itsdigest.com/10-advantages-autonomous-vehicles>
- [3] D. Yadron and D. Tynan, "Tesla driver dies in first fatal crash while using autopilot mode," *Guardian*, vol. 1, 2016. [Online]. Available: <https://www.theguardian.com/technology/2016/jun/30/tesla-autopilot-death-self-driving-car-elon-musk>
- [4] K. Winter, "For self-driving cars, there's big meaning behind one big number: 4 terabytes," Intel Newsroom, Santa Clara, California, Tech. Rep., Jul. 2021, vol. 14. [Online]. Available: <https://www.businesswire.com/news/home/20170414005225/en/Intel-Editorial-For-Self-Driving-Cars-There>
- [5] I. Skog and P. Handel, "In-car positioning and navigation technologies—A survey," *IEEE Trans. Intell. Transp. Syst.*, vol. 10, no. 1, pp. 4–21, Mar. 2009.
- [6] R. Mautz, "Combination of indoor and outdoor positioning," in *Proc. 1st Int. Conf. Mach. Control Guid.*, Zurich, Switzerland, 2008, pp. 1–9.
- [7] K. Ramasubramanian and K. Ramaiah, "Moving from legacy 24 GHz to state-of-the-art 77-GHz radar," *ATZelektronik Worldwide*, vol. 13, no. 3, pp. 46–49, Jun. 2018.
- [8] *Attenuation Due to Clouds and Fog*, document P.840, ITU-R, 2019.
- [9] L. J. Ippolito, "Attenuation by atmospheric gases," in *Radiowave Propagation in Satellite Communications*. Geneva, Switzerland: Springer, 1986, pp. 25–37. [Online]. Available: <https://www.itu.int/rec/R-REC-P.840>
- [10] T. Peynot, J. Underwood, and S. Scheduling, "Towards reliable perception for unmanned ground vehicles in challenging conditions," in *Proc. IEEE/RSJ Int. Conf. Intell. Robots Syst.*, Oct. 2009, pp. 1170–1176.
- [11] J. Wojtanowski, M. Zygmunt, M. Kaszczuk, Z. Mierczyk, and M. Muzal, "Comparison of 905 nm and 1550 nm semiconductor laser rangefinders' performance deterioration due to adverse environmental conditions," *Opto-Electron. Rev.*, vol. 22, no. 3, pp. 183–190, Jan. 2014.
- [12] L. Zhaoyu, G. Chunfeng, W. Zhaoying, J. Dongfang, and Y. Tianxin, "Basics and developments of frequency modulation continuous wave LiDAR," *Opto-Electron. Eng.*, vol. 46, pp. 190038-1–190038-14, Jul. 2019.
- [13] I. Gultepe, R. Tardif, S. C. Michaelides, J. Cermak, A. Bott, J. Bendix, M. D. Müller, M. Pagowski, B. Hansen, G. Ellrod, and W. Jacobs, "Fog research: A review of past achievements and future perspectives," *Pure Appl. Geophys.*, vol. 164, nos. 6–7, pp. 1121–1159, Jun. 2007.
- [14] M. Bijelic, T. Gruber, and W. Ritter, "A benchmark for LiDAR sensors in fog: Is detection breaking down?" in *Proc. IEEE Intell. Vehicles Symp. (IV)*, Jun. 2018, pp. 760–767.
- [15] A. Filgueira, H. González-Jorge, S. Lagüela, L. Díaz-Vilariño, and P. Arias, "Quantifying the influence of rain in LiDAR performance," *Measurement*, vol. 95, pp. 143–148, Jan. 2017.
- [16] J. A. Scheer and J. L. Kurtz, *Coherent Radar Performance Estimation*. Boston, MA, USA: Artech House, 1993.
- [17] S. Haykin, "Cognitive radar: A way of the future," *IEEE Signal Process.*, vol. 23, no. 1, pp. 30–40, Feb. 2006.
- [18] H.-S. Lim, J.-E. Lee, H.-M. Park, and S. Lee, "Stationary target identification in a traffic monitoring radar system," *Appl. Sci.*, vol. 10, no. 17, p. 5838, Aug. 2020.
- [19] D. Felguera-Martín, J.-T. González-Partida, P. Almorox-González, and M. Burgos-García, "Vehicular traffic surveillance and road lane detection using radar interferometry," *IEEE Trans. Veh. Technol.*, vol. 61, no. 3, pp. 959–970, Mar. 2012.
- [20] Z. Xu, J. Zhao, F. Zhang, L. Zhang, T. Yang, Q. Li, and S. Pan, "Photonics-based radar-LiDAR integrated system for multi-sensor fusion applications," *IEEE Sensors J.*, vol. 20, no. 24, pp. 15068–15074, Dec. 2020.
- [21] A. Sharma, S. Chaudhary, J. Malhotra, M. Saadi, S. Al Otaibi, J. Nebhen, and L. Wuttisittikulkiij, "A cost-effective photonic radar under adverse weather conditions for autonomous vehicles by incorporating a frequency-modulated direct detection scheme," *Frontiers Phys.*, vol. 9, p. 467, Sep. 2021.
- [22] S. Chaudhary, L. Wuttisittikulkiij, M. Saadi, A. Sharma, S. Al Otaibi, J. Nebhen, D. Z. Rodriguez, S. Kumar, V. Sharma, G. Phanomchoeng, and R. Chanchaoren, "Coherent detection-based photonic radar for autonomous vehicles under diverse weather conditions," *PLoS ONE*, vol. 16, no. 11, Nov. 2021, Art. no. e0259438.
- [23] A. Sharma and J. Malhotra, "Simulative investigation of FMCW based optical photonic radar and its different configurations," *Opt. Quantum Electron.*, vol. 54, Mar. 2022, Art. no. 233.
- [24] P. Adany, C. Allen, and R. Hui, "Chirped LiDAR using simplified homodyne detection," *J. Lightw. Technol.*, vol. 27, no. 16, pp. 3351–3357, Aug. 15, 2009.
- [25] D. Pierrotet, F. Amzajerjian, L. Petway, B. Barnes, G. Lockard, and M. Rubio, "Linear FMCW laser radar for precision range and vector velocity measurements," *MRS Online Proc. Library*, vol. 1076, 2008. [Online]. Available: <https://ntrs.nasa.gov/api/citations/20080026181/downloads/20080026181.pdf>
- [26] W. Chen, D. Zhu, Z. Chen, and S. Pan, "Full-duty triangular pulse generation based on a polarization-multiplexing dual-drive Mach-Zehnder modulator," *Opt. Exp.*, vol. 24, no. 25, pp. 28606–28612, Dec. 2016.
- [27] Z. Xu, K. Chen, H. Zhang, and S. Pan, "Multifunction LiDAR system based on polarization-division multiplexing," *J. Lightw. Technol.*, vol. 37, no. 9, pp. 2000–2007, May 1, 2019.
- [28] C. J. Karlsson and F. Olsson, "Linearization of the frequency sweep of a frequency-modulated continuous-wave semiconductor laser radar and the resulting ranging performance," *Appl. Opt.*, vol. 38, no. 15, pp. 3376–3386, 1999.
- [29] A. H. Elghandour and C. D. Ren, "Modeling and comparative study of various detection techniques for FMCW LiDAR using optisystem," *Proc. SPIE*, vol. 8905, Sep. 2013, Art. no. 890529.
- [30] P. Zhou, F. Zhang, and S. Pan, "Generation of linear frequency-modulated waveforms by a frequency-sweeping optoelectronic oscillator," *J. Lightw. Technol.*, vol. 36, no. 18, pp. 3927–3934, Sep. 15, 2018.
- [31] G. P. Agrawal, *Fiber-Optic Communication Systems*, vol. 222. Hoboken, NJ, USA: Wiley, 2012.
- [32] R. Hui and M. O'Sullivan, *Fiber Optic Measurement Techniques*. New York, NY, USA: Academic, 2009.
- [33] G. Keiser, *Optical Communications Essentials*. New York, NY, USA: McGraw-Hill, 2003.
- [34] F. Rashidia, J. He, and L. Chena, "Spectrum slicing WDM for FSO communication systems under the heavy rain weather," *Opt. Commun.*, vol. 387, pp. 296–302, Mar. 2017.
- [35] R. Olsen, D. Rogers, and D. Hodge, "The aRbrelation in the calculation of rain attenuation," *IEEE Trans. Antennas Propag.*, vol. AP-26, no. 2, pp. 318–329, Mar. 1978.
- [36] L. Yangang, "Statistical theory of the marshall-palmer distribution of raindrops," *Atmos. Environ. A, Gen. Topics*, vol. 27, no. 1, pp. 15–19, Jan. 1993.
- [37] K. Anbarasi, C. Hemanth, and R. G. Sangeetha, "A review on channel models in free space optical communication systems," *Opt. Laser Technol.*, vol. 97, pp. 161–171, Dec. 2017.
- [38] M. S. Awan, L. Csurgai-Horváth, S. S. Muhammad, E. Leitgeb, F. Nadeem, and M. S. Khan, "Characterization of fog and snow attenuations for free-space optical propagation," *J. Commun.*, vol. 4, no. 8, pp. 533–545, Sep. 2009.
- [39] M. S. Awan, Marzuki, E. Leitgeb, B. Hillbrand, F. Nadeem, and M. S. Khan, "Cloud attenuations for free-space optical links," in *Proc. Int. Workshop Satell. Space Commun.*, Sep. 2009, pp. 274–278.
- [40] F. Zhang, Q. Guo, and S. Pan, "Photonics-based real-time ultra-high-range-resolution radar with broadband signal generation and processing," *Sci. Rep.*, vol. 7, no. 1, p. 13848, Dec. 2017.
- [41] G. Serafino, F. Amato, S. Maresca, L. Lembo, P. Ghelfi, and A. Bogoni, "Photonic approach for on-board and ground radars in automotive applications," *IET Radar, Sonar Navigat.*, vol. 12, no. 10, pp. 1179–1186, Oct. 2018.

- [42] L. Lembo, S. Maresca, G. Serafino, F. Scotti, F. Amato, P. Ghelfi, and A. Bogoni, "In-field demonstration of a photonic coherent MIMO distributed radar network," in *Proc. IEEE Radar Conf. (RadarConf)*, Boston, MA, USA, Apr. 2019, pp. 1–6.
- [43] V. Sharma and S. Sergeyev, "Range detection assessment of photonic radar under adverse weather perceptions," *Opt. Commun.*, vol. 472, Oct. 2020, Art. no. 125891.
- [44] Y. Wang, X. Hou, T. Li, Z. He, D. Wang, F. Yang, T. Zhou, and L. Rong, "Simultaneous detection of the distance and direction for a noncooperative target based on the microwave photonic radar," *Opt. Exp.*, vol. 29, pp. 31561–31573, 2021.
- [45] S. Fang, G. Li, F. Zhang, B. Han, and W. Hong, "A novel scheme for processing FMCW-ladar data acquired with low sampling rate," *Geo-Spatial Inf. Sci.*, pp. 1–11, Mar. 2022.
- [46] D. Liang, L. Jiang, and Y. Chen, "Multi-functional microwave photonic radar system for simultaneous distance and velocity measurement and high-resolution microwave imaging," *J. Lightw. Technol.*, vol. 39, no. 20, pp. 6470–6478, Oct. 15, 2021.



AMIR PARNIANIFARD received the Ph.D. degree from the Faculty of Mechanical and Manufacturing Engineering, University Putra Malaysia, in January 2019. Since February 2020, he has been working as a Research Assistant (Postdoctoral Fellow) with the Faculty of Engineering, Chulalongkorn University, Bangkok, Thailand. He is also a PMP R certified from the Project Management Institute (PMI), USA. His research interests include computational intelligence using surrogate-based simulation-optimization with an approach to the analysis of computer experiments, adaptive improvement, robust black-box optimization, and its application in practical engineering design problems under uncertainty, such as robot manipulators, control systems, and wireless communications.



and wireless communication

ABHISHEK SHARMA (Graduate Student Member, IEEE) received the B.E. degree from the SLIET University and the M.Tech. degree from Punjab Technical University. He is currently pursuing the Ph.D. degree with the Faculty of Engineering and Technology, Guru Nanak Dev University, Amritsar. He has ten years of experience of teaching. His research interests include free space optics, radio over free space optics, spatial division multiplexing, hybrid optical and wireless communication systems, and photonics surveillance schemes.



SUSHANK CHAUDHARY (Senior Member, IEEE) received the Ph.D. degree from the Universiti Utara Malaysia, Sintok, Malaysia. During 2018–2020, he was associated as a Postdoctoral Researcher with the Fujian Institute of Research on Structure and Matter, Chinese Academy of Sciences. He is currently associated with Chulalongkorn University, Bangkok, Thailand. He has published more than 70 research papers in SCI, Scopus international journals, and international conferences. His main research interests include autonomous vehicles, photonic radars, spatial division multiplexing, free space optics, and visible light communication systems. In 2019, he was awarded an Elite Talent Award from Jinjiang Government, China. He has delivered keynote speeches in Technology Transfer Summit, Jinan, China, and the IEEE International Conference on Signal Processing and Integrated Networks, SPIN 2020 held at Noida, India.



JYOTEESH MALHOTRA received the M.Tech. and Ph.D. degrees. He has more than 20 years of experience of teaching and research. He is currently an Associate Dean of Academics of Student Welfare, a Professor, and the Head of the Department of Electronics and Communication Engineering and the Department of Computer Science and Engineering in the Regional Campus Jalandhar, Guru Nanak Dev University, Amritsar. He has more than 175 publications in journals of international and national repute in his credit. His research interests include wireless networks and optical communication. He received the Gold Medal for his M.Tech. degree.



SANTOSH KUMAR (Senior Member, IEEE) received the Ph.D. degree from IIT (ISM) Dhanbad, Dhanbad, India. He is currently an Associate Professor with the School of Physics Science and Information Technology, Liaocheng University, Liaocheng, China. He is also a Traveling Lecturer of OPTICA. He has guided seven M.Tech. dissertations and six Ph.D. candidates. He has published more than 190 research papers in national and international SCI journals and conferences. He has presented many articles at conferences held in Belgium and USA. He has published two books entitled *Fibre Optic Communication: Optical Waveguides, Devices and Applications* (University Press, 2017), India, and another book entitled *2D Materials for Surface Plasmon Resonance-Based Sensors* (CRC Press, Taylor & Francis Group, 2021). He has reviewed more than 920 SCI journals of IEEE, Elsevier, Springer, OPTICA, SPIE, and Nature. His current research interests include optical fiber sensors, nano and biophotonics, photonic and plasmonic devices, and waveguide and interferometer. He is a Life Fellow of the Optical Society of India (OSI) and a Senior Member of OPTICA and SPIE. He is also the Chair of the Optica Optical Biosensors Technical Group. He has delivered many invited talks and serves as the session chair for IEEE conferences. He is also an Associate Editor of the IEEE SENSORS JOURNAL, IEEE ACCESS, IEEE TRANSACTIONS ON NANOBIOSCIENCE, and *Biomedical Optics Express*.



LUNCHAKORN WUTTISITTIKULKIJ (Senior Member, IEEE) received the B.Eng. degree in electrical engineering from Chulalongkorn University, Bangkok, Thailand, in 1990, and the M.Sc. and Ph.D. degrees in telecommunications from the University of Essex, U.K., in 1992 and 1997, respectively. In 1995, he was involved with the European Commission Funded Project, such as Multiwavelength Transport Network (MWTN) responsible for network design and dimensioning. In 1997, he joined the Faculty of Engineering, Chulalongkorn University, where he is currently an Associate Professor with the Department of Electrical Engineering. He has authored 13 books and over 50 research articles. His research interest includes broadband wireless access networks.

...